Alcohol Attenuates CRF-Induced Excitatory Effects from the Extended Amygdala to Dorsostriatal Cholinergic Interneurons

Amanda Essoh[1,#], Xueyi Xie[1,#], Himanshu Gangal[1], Zhenbo Huang[1], Ruifeng Chen[1], Ziyi Li[1], Xuehua Wang[1], Valerie Vierkant[1], Miguel Garza[1], Lierni Ugartemendia[2], Maria E. Secci[3], Nicholas W. Gilpin[3], Nicholas J. Justice[2], Robert O. Messing[4] and Jun Wang[1]*

[1]Department of Neuroscience and Experimental Therapeutics, College of Medicine, Texas A&M University Health Science Center, Bryan, Texas 77807

[2]Center for Metabolic and Degenerative Disease, Institute of Molecular Medicine, University of Texas, Houston, Texas 77030

[3]Department of Physiology, Louisiana State University Health Sciences Center, New Orleans, Louisiana, 70112

[4]Department of Neuroscience, University of Texas, Austin, Texas, 78712

[#]These authors contributed equally

Running Title: Extended Amygdala–Striatum CRF Circuit Altered by Alcohol

Key Words: CRF and CRFR1, alcohol/ethanol, dorsal striatum, CeA, BNST, cholinergic interneuron, stress, Acetylcholine (ACh), slice electrophysiology, neurocircuit tracing

*To whom correspondence should be addressed:
Jun Wang, M.D., Ph.D.
2106 Medical Research and Education Building
8447 John Sharp Pkwy, Bryan, TX 77807
Tel: 979-436-0389 Fax: 979-436-0086 E-mail: jwang188@tamu.edu

Pages: 34, Figures: 6, Abstract: 182 words, Introduction: 348, Discussion: 514

Abstract

Alcohol relapse is associated with corticotropin-releasing factor (CRF) signaling and altered reward pathway function, though the precise mechanisms remain unclear. Here, we investigated how CRF modulates cholinergic interneurons (CINs) in the dorsal striatum, a region critical in mediating cognitive flexibility and action selection. Using monosynaptic and retrograde circuit tracing, we identified direct inputs from CRF-expressing (CRF^+) neurons in the central amygdala (CeA) and bed nucleus of the stria terminalis (BNST) to dorsal striatal CINs. We showed that CINs express CRF receptor 1 (CRFR1) and established their functional connectivity with CeA/BNST CRF^+ projections. Functional recordings revealed that CRF enhanced CIN excitability and promoted acetylcholine release in the dorsal striatum. However, acute alcohol exposure and withdrawal attenuated the excitatory effect of CRF on CIN firing, suggesting a mechanism by which alcohol disrupts CRF-dependent neuromodulation. These findings reveal a previously unrecognized CRF-CIN pathway linking the extended amygdala to the dorsal striatum and provide new insight into how CRF and alcohol interact to impair striatal function. This work highlights CRF signaling as a potential target for understanding stress-induced changes to the reward pathway.

Highlights

- Dorsal striatal CINs receive monosynaptic CRF^+ inputs from CeA and BNST neurons.
- CRFR1 is expressed in striatal CINs, and CRF^+ fibers are present in the dorsal striatum.

- CRF enhances dorsal striatal CIN activity via CRFR1 signaling.
- Acute alcohol exposure impairs CRF-induced cholinergic activity.

Significance Statement

The dorsal striatum regulates goal-directed behavior and is implicated in alcohol use disorder (AUD). Within this region, cholinergic interneurons (CINs) support cognitive flexibility and receive input from limbic areas, including the central amygdala (CeA) and bed nucleus of the stria terminalis (BNST). In this study, we identified direct projections from CRF-producing neurons in the CeA and BNST to dorsal striatal CINs, a subset of which express CRF receptor 1 (CRFR1). Electrophysiological recordings confirmed these projections provide functional input that is disrupted by acute alcohol exposure. These findings lay the groundwork for future studies on how CRF and alcohol interact to impair striatal function.

63 **Introduction**

64 Alcohol use disorder (AUD) is a chronic, relapsing brain condition affecting over
65 14 million adults in the U.S., characterized by compulsive alcohol consumption, impaired
66 control over drinking, and negative emotional states during withdrawal. Stress is a key
67 contributor to both the development and recurrence of AUD, with stressful experiences
68 and elevated stress hormone levels frequently precipitating relapse episodes in abstinent
69 individuals [1-3]. An expanding body of clinical and preclinical evidence highlights the
70 importance of stress-responsive neurocircuits in driving addiction-related behaviors,
71 implicating neuropeptides like corticotropin-releasing factor (CRF) in relapse vulnerability
72 [4-8]. CRF is a central regulator of the stress response, coordinating hormonal and
73 behavioral adaptations to stress through widespread action in both hypothalamic and
74 extrahypothalamic brain regions. In addition to initiating hypothalamic-pituitary-adrenal
75 (HPA) axis activity, CRF modulates affective and motivational processes through its
76 action within the amygdala, bed nucleus of the stria terminalis (BNST), and other limbic
77 structures.

78 Substantial evidence indicates that CRF signaling promotes drug-seeking
79 behavior during stress and withdrawal across multiple substances of abuse, supporting
80 its role as a critical mediator of relapse [5, 6, 9]. Despite extensive research on CRF in
81 limbic areas, its role in the dorsal striatum, an area crucial for habit formation and
82 behavioral flexibility, remains less well understood [10-16]. Within this region, cholinergic
83 interneurons (CINs) are key regulators of striatal output and acetylcholine (ACh)-
84 mediated dopamine modulation, integrating diverse inputs and contributing to reward-
85 based learning [17-19]. CINs are sensitive to neuromodulatory influences, yet it is unclear

86 whether they are directly targeted by CRF and how this interaction might be altered by
87 alcohol exposure [20-22].

88 In this study, we investigated a novel CRF-CIN circuit linking the CeA and BNST
89 to the dorsal striatum. Using monosynaptic and retrograde circuit tracing, we identified
90 direct projections from CRF-expressing neurons to dorsal striatal CINs. CRF enhanced
91 CIN excitability and promoted ACh release via CRFR1 activation, but this excitatory effect
92 was disrupted by acute alcohol exposure, indicating that alcohol interferes with CRF-
93 dependent cholinergic modulation. These findings identify a CRF-CIN circuit that is
94 vulnerable to alcohol-induced dysregulation, providing mechanistic insight into how stress
95 peptides and alcohol interact to impair striatal function.

96

97 **Materials and Methods**

98 **Animals**

99 Male and female 3-4-month-old mice or rats were used in all studies. Rats were
100 mainly used for histological validation of CRFR1 expression with the CRFR1-Cre-
101 tdTomato line, whereas mice were used for histology, electrophysiology, optogenetics,
102 and GRAB-ACh sensor experiments because of the availability of transgenic Cre-driver
103 and reporter lines. ChAT-eGFP (stock 007902), ChAT-Cre (stock 031661), Drd1a-
104 tdTomato (D1-tdT, stock 016204), Ai32 (stock 012569), CRH-ires-CRE (stock 012704)
105 and C57BL/6J (stock 000664) mice were purchased from The Jackson Laboratory [23-
106 27]. CRFR1-GFP mice were gifted by Dr. Marisa Roberto's lab. All mice were backcrossed
107 onto a C57BL/6 background. ChAT-Cre mice were crossed with D1-tdTomato mice to
108 obtain ChAT-Cre;D1-tdTomato mice. CRF-Cre mice were crossed with ChAT-eGFP mice

109 to generate CRF-Cre;ChAT-eGFP mice. CRF-Cre;Ai32 mice were generated in-house
110 and crossed with ChAT-eGFP to generate triple transgenic CRF-Cre;Ai32;ChAT-eGFP
111 mice. We used CRFR1-Cre-2A-tdTomato rats that have been validated for expression of
112 Cre and tdTomato in CRFR1-expressing neurons [28]. We also used CRF-Cre rats that
113 have been shown to express Cre recombinase in CRF-producing neurons in the CeA and
114 BNST [29]. We crossed CRF-Cre rats with a Cre-dependent tdTomato reporter line to
115 visualize CRF^+ neurons. Genotypes were confirmed through PCR analysis of tail DNA to
116 detect Cre or fluorescent protein genes in mice and rats (Cre for CRF-Cre and ChAT-Cre,
117 tdTomato for D1-tdTomato, and GFP for Ai32) [30-34]. Animals were housed in a
118 temperature- and humidity-controlled vivarium with a 12-h light/dark cycle. Food and
119 water were available *ad libitum*. The Texas A&M University Institutional Animal Care and
120 Use Committee approved all animal care and experimental procedures.

121 **Reagents**

122 AAV8-Ef1a-FLEX-TVA-mCherry (lot # AV5008b), AAV8-FLEX-RG (lot # AV5005f),
123 and AAV-FLEX-Chrimson-tdTomato (lot # AV5844) were purchased from the UNC Vector
124 Core [35, 36]. AAVrg-pCAG-FLEX-eGFP-WPRE (catalog # 51502-AAVrg) was purchased
125 from Addgene [37], while EnvA-SADΔG-GFP was purchased from the Salk Institute [38].
126 Choline acetyltransferase (AB144P) antibody was purchased from Sigma [39]. ACh
127 sensor (AAV-$GRAB_{ACh4m}$) was obtained from BrainVTA (PT-7021) [40-44], which is an
128 updated version of ACh3.0 [45]. CRF peptide and NBI 35695 (CRFR1 antagonist) were
129 obtained from Tocris. 6,7-dinitroquinoxaline-2,3-dione (DNQX), tetrodotoxin (TTX), 4-
130 aminopyridine (4-AP), and bicuculline were also purchased from Tocris.

131 **Stereotaxic virus infusion**

132 The stereotaxic virus infusion procedure was conducted as described previously
133 [30, 46, 47]. When required for the experimental design, AAV-DIO-TVA-mCherry and AAV-
134 DIO-RG were bilaterally infused into the dorsomedial striatum (AP: 0.38 mm, ML: ±1.55
135 mm, DV: -2.90 mm from the Bregma) [48] of ChAT-Cre;D1-tdTomato mice (Fig. 1).
136 Rabies-GFP was infused at the same injection site three weeks later at a 10-degree angle
137 to avoid contamination of the infusion tract. Rabies-GFP virus was allowed to incubate for
138 one week. AAVrg-pCAG-FLEX-eGFP-WPRE was infused into the dorsal striatum (AP:
139 0.00, mm, ML: ±2.80 mm, DV: -4.85 mm from the Bregma) [49, 50] of CRF-Cre;tdTomato
140 rats (Fig. 3A-3E). Additionally, AAV-DIO-Chrimson-tdTomato was infused into the CeA (AP:
141 -1.60 mm; ML: ±4.20 mm; DV: -8.10 mm) and BNST (AP: -0.10 mm; ML: ±1.40 mm; DV:
142 -6.70 mm) of CRF-Cre;ChAT-GFP mice as described in published literature [51] (Fig. 3F-
143 3H). The animals were placed on a stereotaxic surgical frame after being sedated with 3-
144 4% isoflurane at a rate of 1.0 L/min, as described previously [46, 47, 52]. These
145 coordinates were obtained from previous publications and verified using the rat [53] or
146 mouse [54] brain atlases. A volume of 0.5 μL/site (mice) or 1 μL/site (rats) of virus was
147 infused at a rate of 0.08 μL/min. At the end of the infusion, the injectors remained at the
148 injection site for 10 to 15 min before removal to allow for virus diffusion. The scalp incision
149 was then sutured and animals were returned to their home cage for recovery.

150 **Histology and cell counting**

151 Animals were anesthetized and perfused intracardially with 4% paraformaldehyde
152 (PFA) in phosphate-buffered saline (PBS). The brains were extracted and submerged in
153 4% PFA/PBS solution for one day at 4°Cbefore being transferred to a 30% sucrose
154 solution in PBS. Once the brains completely sank in the sucrose solution, they were cut

155 into 50-μm thick coronal sections using a cryostat. The slices were stored in a PBS bath
156 at 4°C before mounting on slides for imaging using a confocal laser-scanning microscope
157 (Fluoview, Olympus). All images were processed using Imaris 8.3.1 (Bitplane, Zurich,
158 Switzerland) as previously reported [30, 32, 34]. Immunostaining for choline
159 acetyltransferase (ChAT) was performed using an anti-ChAT primary antibody (AB144P),
160 followed by a fluorophore-conjugated secondary antibody (A21447) emitting at 647 nmto
161 label CINs with far-red fluorescence. Cell counting was performed in 8 CRF-Cre;tdTomato
162 rats. For each brain region, 5-10 brain sections were imaged from each animal. Imaris
163 was used to quantify green and red neurons as well as evaluate colocalization. Brain
164 regions were identified using the Mouse Brain Atlas [54]. Images were primarily obtained
165 from the posterior dorsomedial striatum, corresponding to coronal slices posterior to the
166 crossing of the anterior commissure and anterior to the tail of the striatum (starting around
167 0.62 mm and ending at −1.3 mm relative to the Bregma).

168 **Slice electrophysiology**

169 ***Slice preparation.*** Slices were prepared and electrophysiological recordings were
170 conducted as described previously [30, 32, 46, 47, 55]. Briefly, coronal sections (250 μm)
171 containing the posterior dorsomedial striatum were cut in an ice-cold cutting solution
172 containing (in mM): 40 NaCl, 148.5 sucrose, 4 KCl, 1.25 NaH_2PO_4, 25 $NaHCO_3$, 0.5 $CaCl_2$,
173 7 $MgCl_2$, 10 glucose, 1 sodium ascorbate, 3 sodium pyruvate, and 3 myo-inositol. The
174 solution was saturated with 95% O_2 and 5% CO_2. Slices were then incubated in a 1:1
175 mixture of the cutting and external solutions at 32°C for 45 min. The external solution was
176 composed of the following (in mM): 125 NaCl, 4.5 KCl, 2.5 $CaCl_2$, 1.3 $MgCl_2$, 1.25
177 NaH_2PO_4, 25 $NaHCO_3$, 15 glucose, and 15 sucrose. The external solution was saturated

178 with 95% O_2 and 5% CO_2. Slices were then maintained in the external solution at room
179 temperature until use. Recordings were primarily obtained from the posterior dorsomedial
180 striatum, corresponding to coronal slices posterior to the crossing of the anterior
181 commissure and anterior to the tail of the striatum (starting around 0.62 mm and ending
182 at −1.3 mm relative to the Bregma). More anterior slices were occasionally included to
183 increase the sample size.

184 ***Cell-attached recordings.*** Individual slices were transferred to a recording chamber and
185 continuously perfused with the external solution at 2-3 mL/min at 32°C. Fluorescent
186 axonal fibers and neurons were visualized using an epifluorescence microscope
187 (Olympus). The presence of tdTomato and GFP allowed cell type verification and
188 expression of Ai32 allowed visualization of CRF-producing fibers. CINs in slices were
189 identified by their labeled color, large size, and spontaneous firing. Spontaneous cell-
190 attached CIN firing activity was recorded for 5 min to calculate the average firing
191 frequency. Light at 470-nm or 590-nm light was **delivered** from the objective lens for 2
192 ms at frequencies and durations specified in the figure legends to stimulate
193 channelrhodopsin-expressing axonal fibers in the dorsal striatum. We used a potassium-
194 based intracellular solution containing (in mM): 123 potassium gluconate, 10 HEPES, 0.2
195 EGTA, 8 NaCl, 2 MgATP, and 0.3 NaGTP, with an osmolarity of ~280 mOsm/L and the
196 pH adjusted to 7.3 using KOH. For protocols involving alcohol application, we pretreated
197 dorsal striatal slices with alcohol (50 mM) for 1 h outside of the recording chamber. After
198 pretreatment, slices were transferred to the recording chamber, where alcohol was
199 washed out for at least 15 min before recording. The recordings included a 10-minute
200 baseline period (without alcohol), followed by 10 minutes of CRF bath application and 10

201 minutes of alcohol exposure. Control slices did not receive alcohol pretreatment but were
202 exposed to acute alcohol following CRF application. In both conditions, the final 10-min
203 alcohol application allowed us to assess whether alcohol pretreatment altered the CIN
204 firing response to subsequent CRF and alcohol exposure. In protocols that required
205 inhibition of glutamatergic and $GABA_A$ receptors, DNQX and bicuculline were used,
206 respectively. Electrophysiology data were acquired using Clampex-10 (Molecular Devices)
207 and analyzed using Clampfit-10 (Molecular Devices) and Mini Analysis (Mini60,
208 Synaptosoft Inc.).

209 **Ex vivo live-tissue confocal imaging of ACh release**

210 Brain slices were kept in a recording chamber perfused with oxygenated external
211 solution (95% O_2 and 5% CO_2). An Olympus FluoView FV3000 microscope was used with
212 a 10x NA 0.3 and a 40x NA 0.8 water immersion objective, along with a 488 nm and a
213 561 nm laser. The sample rate of imaging was 2 to 3 frames per second. Parameters
214 were maintained consistently across all imaging sessions, including laser intensity, HV,
215 gain, offset, and aperture diameter.

216 **Statistical analysis**

217 Before conducting all experiments shown in this study, we performed a power analysis
218 with SigmaPlot software (12.5, Systat) using the mean and standard deviation from
219 previous studies in our lab [34, 48-50] to determine the required sample sizes to detect a
220 significant difference. We tested all data for normality before significance testing. If the
221 normality test failed, we used nonparametric tests, such as the Mann-Whitney U Test. All
222 data are expressed as mean ± SEM. Data were analyzed by two-tailed *t*-test (unpaired or
223 paired), one- or two-way ANOVA with repeated measures, followed by the Tukey or Sidak

post hoc test. Significance was determined if $p < 0.05$. Statistical analysis was conducted by the SigmaPlot program. Graphs were constructed using the OriginPro (2024b, OriginLab) program.

Results

Dorsal Striatal CINs Receive Monosynaptic Inputs from CeA and BNST Neurons

To investigate the connection between dorsal striatal CINs and stress-related brain regions, we examined whether CINs receive monosynaptic inputs from the CeA and the BNST [56, 57]. We used ChAT-Cre;D1-tdTomato mice to perform rabies-mediated monosynaptic retrograde tracing. In this mouse model, CINs express Cre recombinase, and dopamine D1-receptor (D1R)-expressing medium spiny neurons (D1-MSNs) are labeled with tdTomato. Including the D1-tdTomato marker allowed us to delineate the CeA and BNST, which, unlike surrounding striatal areas, do not express D1Rs [52]. We performed rabies-mediated retrograde monosynaptic circuit tracing (Fig. 1A), allowing specific targeting of CINs (Fig. 1B). In addition to labeling neurons in brain regions known to project to dorsal striatal CINs—including the striatum itself, cortex (e.g., cingulate cortex, motor cortex, somatosensory cortex), thalamus (e.g., parafascicular thalamic nucleus, centrolateral thalamic nucleus), globus pallidus, and midbrain—we were surprised to see labeled neurons in both the CeA (Fig. 1C) and BNST (Fig. 1D), which are well-characterized as key stress-responsive nuclei. Interestingly, the BNST had a higher density of DMS-projecting neurons than the CeA (Fig 1E; Mann-Whitney U = 4.000, ***$p < 0.001$). These results demonstrate that dorsal striatal CINs receive direct, monosynaptic inputs from neurons in the CeA and BNST. Together, these findings

247 highlight the anatomical connection of dorsal striatal CINs with key stress-responsive
248 brain regions.
249

250 **The Dorsal Striatum Lacks CRF$^+$ Neurons Unlike the CeA and BNST**

251 We first investigated whether the dorsal striatum contains CRF-producing cells or
252 whether CRF signaling in this region depends on CeA and BNST inputs. While previous
253 studies have identified CRF-producing neurons in the CeA and BNST [51], their presence
254 in the dorsal striatum was uncertain. Coronal brain sections from CRF-Cre;tdTomato rats
255 revealed dense populations of CRF-tdTomato$^+$ neurons in the CeA (Fig. 2A) and BNST
256 (Fig. 2B). Although CRF$^+$ axonal fibers were observed in the dorsal striatum, CRF$^+$ cell
257 bodies were largely absent (Fig. 2C). Quantitative analysis confirmed significant regional
258 differences, indicating that the CeA and BNST contained substantially more CRF$^+$
259 neurons than the dorsal striatum (Fig. 2D; CeA versus DS, Q = 6.62, $^*p < 0.05$; BNST
260 versus DS, Q = 4.54, $^*p < 0.05$). Notably, the CeA exhibited a similar density of CRF$^+$
261 neurons to the BNST (Fig. 2D; Q = 1.40, $p > 0.05$). The apparent lack of CRF$^+$ cell bodies
262 suggests that CRF signaling in the dorsal striatum originates from CRF$^+$ neurons in the
263 CeA and BNST.
264

265 **Dorsal Striatum CINs Receive Monosynaptic CRF$^+$ Inputs from the CeA and BNST**

266 To test whether CRF$^+$ neurons in the CeA and BNST project to the dorsal striatum,
267 we infused a retrograde adeno-associated virus into the dorsal striatum of CRF-
268 Cre;tdTomato rats. This strategy labels CRF$^+$ neurons (tdTomato$^+$) that project to the
269 dorsal striatum with GFP (Fig. 3A). Confocal imaging revealed GFP$^+$ neurons in both the

270 BNST (Fig. 3B) and CeA (Fig. 3C), with substantial overlap between GFP-labeled dorsal
271 striatum-projecting neurons and tdTomato-positive (CRF^+) cells in both regions. This
272 indicates that CRF^+ neurons from the CeA and BNST project to the dorsal striatum.
273 Despite a similar overall CRF^+ neuron density in the CeA and BNST (Fig. 3D; $t_{15} = 1.06$,
274 $p > 0.05$), the proportion of dorsal striatum-projecting CRF^+ neurons was significantly
275 higher in the BNST than in the CeA (Fig. 3E; $t_{15} = -5.01$, ***$p < 0.001$). The density of
276 dorsal striatum-projecting CRF^+ neurons was also higher in the BNST than the CeA (Fig.
277 3F; $t_{15} = -3.07$, **$p < 0.01$). These results indicate that CRF^+ neurons in the CeA and
278 BNST project to the dorsal striatum.

279 To test whether CRF^+ neurons in the CeA and BNST make monosynaptic
280 projections to dorsal striatal CINs, we performed opsin-assisted functional circuit tracing.
281 Given that both the CeA and BNST are primarily GABAergic nuclei [58, 59], we examined
282 whether optogenetic stimulation of CRF-containing projections to the dorsal striatum
283 induces inhibitory monosynaptic currents in CINs. To test this, we infused AAV-FLEX-
284 Chrimson-tdTomato into the CeA and BNST of CRF-Cre;ChAT-eGFP mice so that we
285 could selectively stimulate CRF-containing fibers in the dorsal striatum while recording
286 from GFP-labeled CINs (Fig. 3G). We found that optogenetic stimulation of CRF^+ fibers
287 with yellow light evoked fast synaptic currents (within ~6.5 ms from the stimulation onset)
288 in dorsal striatal CINs (Fig. 3H-3J). This response was abolished by TTX (Fig. 3H, 3I; $X^2(3)$
289 $= 21.9$, $p < 0.001$; BL versus TTX: $z = 3.10$, *$p < 0.05$) but restored using TTX+4-AP (Fig.
290 3H, 3I; TTX vs TTX+4-AP: $z = 4.26$, ***$p < 0.001$), suggesting the existence of
291 monosynaptic transmission. Notably, the restored synaptic response was predominantly
292 blocked by the $GABA_A$ receptor antagonist bicuculline (Fig. 3H, 3I; TTX+4-AP versus

293 TTX+4-AP+Bic: z = 3.10, *$p < 0.05$), demonstrating that evoked currents are GABAergic.
294 Together, these results demonstrate that dorsal striatal CINs receive monosynaptic
295 GABAergic inputs from CRF^+ neurons in the CeA and BNST, suggesting that these
296 neurons project to the dorsal striatum and may release CRF to modulate cholinergic
297 signaling.
298

299 **Striatal CINs Express CRFR1**

300 Having established that CINs receive monosynaptic inputs from CRF^+ neurons in
301 the CeA and BNST, we next sought to confirm that CINs express the CRF receptor
302 CRFR1 [15, 60, 61]. To address this, we used CRFR1-Cre-tdTomato rats [28], in which
303 CRFR1-expressing neurons express Cre recombinase and are visualized via tdTomato
304 fluorescence. Confocal imaging of striatal sections from these rats confirmed that CRFR1-
305 expressing neurons are distributed throughout the striatum (Fig. 4A). To verify that
306 CRFR1-positive ($CRFR1^+$) neurons are also cholinergic, we stained sections with an anti-
307 ChAT antibody and acquired confocal images (Fig. 4A). We found that ~25% of rat CINs
308 express CRFR1 (Fig. 4B, 4C; Mann-Whitney U = 0.00, ***$p < 0.001$). To determine
309 whether this expression pattern is conserved across species, we examined CRFR1-GFP
310 mice and performed ChAT immunostaining on striatal sections (Fig. 4D). We found that
311 approximately 10% of CINs expressed CRFR1 (Fig. 4E), indicating that while the
312 proportion is lower than in rats, a subset of CINs in both species express CRFR1. These
313 findings align with previous reports showing that a subset of striatal CINs express CRFR1,
314 supporting a role for CRFR1-mediated signaling in the striatum.
315

316 **CRF Enhances CIN Activity and Acetylcholine Release in the Dorsal Striatum**

317 Following the finding that CRF^+ neurons send inputs to the dorsal striatum, we next
318 investigated how CRF influences spontaneous CIN firing activity. Cell-attached
319 recordings of GFP^+ neurons in the dorsal striatum were conducted in ChAT-eGFP mice
320 before and during bath application of CRF (100 nM) (Fig. 5A). We found that CRF
321 significantly increased CIN firing frequency (Fig. 5B, 5C; $t_{(8)} = -24.08$, ***$p < 0.001$). This
322 effect was abolished by pretreatment with the CRFR1 antagonist NBI 35695 (Fig. 5C;
323 Mann-Whitney U = 0.00, ***$p < 0.001$), confirming that CRF potentiates CIN firing via
324 CRFR1 activation in the dorsal striatum.

325 Because CINs are the primary source of ACh in the dorsal striatum, we next
326 examined whether CRF-induced CIN activation modulates ACh release. To do so, we
327 infused an adeno-associated virus (AAV) introducing a genetically encoded ACh sensor
328 (AAV-hSyn-$GRAB_{ACh4m}$) into the dorsal striatum of wildtype mice [40-45]. Live-tissue
329 confocal imaging was performed on brain slices containing the dorsal striatum 14 days
330 post-infusion to monitor ACh levels (Fig. 5D). Bath application of CRF produced a robust
331 ACh fluorescence signal (Fig. 5E, 5F; Mann-Whitney U = 7.00, *$p < 0.05$), indicating that
332 CRF enhances ACh release. These results suggest that CRF-driven CIN activation
333 increases ACh release in the dorsal striatum.

334 To further determine whether direct activation of CRF-expressing fibers modulates
335 CIN activity, we used an optogenetic approach. We generated CRF-Cre;Ai32;ChAT-
336 eGFP mice to selectively stimulate CRF^+ terminals in the dorsal striatum. Cell-attached
337 recordings were conducted in CINs while blue light (470 nm, 50 Hz, 60 s) activated local
338 ChR2-expressing CRF^+ fibers (Fig. 5G). Burst stimulation of CRF^+ terminals significantly

339 and reversibly increased CIN firing in the presence of DNQX and bicuculline (Fig. 5H, 5I;
340 pre vs. stim, q = 3.69, *p < 0.05; stim vs. post, q = 11.82, ***p < 0.001). However,
341 application of a CRFR1 antagonist abolished this effect (Fig. 5J, 5K; $F_{(2,16)}$ = 0.96, p =
342 0.41), confirming that the increase in CIN firing was mediated by CRFR1 signaling.
343 Together, these findings demonstrate that CRF enhances CIN activity and ACh release
344 in the dorsal striatum.
345

346 **Acute Alcohol Application Attenuates CRF-Mediated Enhancement of CIN Firing**

347 Given that acute alcohol exposure suppresses CIN activity [20], we next examined
348 how acute alcohol application and subsequent withdrawal influence CRF-mediated
349 enhancement of CIN firing. We first assessed the effect of acute alcohol by measuring
350 spontaneous CIN activity before, during, and after 50 mM alcohol application in dorsal
351 striatal slices from ChAT-eGFP mice. Consistent with previous reports [20], acute alcohol
352 significantly suppressed CIN spontaneous firing, an effect reversed after a washout
353 period, which we refer to here as withdrawal (Fig. 6A, 6B; Mann-Whitney U = 0.00, *p <
354 0.05).

355 To determine how prior alcohol exposure (modeling early withdrawal) affects CRF-
356 induced enhancement of CIN firing, we pretreated dorsal striatal slices with alcohol (50
357 mM) for 1 h outside of the recording chamber (Fig. 6C), followed by CRF application
358 during recordings. In untreated control slices, CRF significantly increased spontaneous
359 CIN firing, consistent with our previous findings (Fig. 6D; BL versus CRF, q = 11.51, ***p
360 < 0.001; see also Fig. 5B). When alcohol was subsequently applied after CRF, firing
361 decreased but remained elevated relative to baseline (Fig. 6D; CRF versus EtOH, q =

362 6.21, $^{**}p < 0.01$; BL versus EtOH, q = 5.29, $^{**}p < 0.01$), likely due to a residual CRF effect
363 (Fig. 5B).
364 In slices pretreated with alcohol (mimicking early withdrawal), CRF still increased
365 CIN firing, but subsequent alcohol application did not fully return firing to baseline levels
366 (Fig. 6E; BL versus CRF, q = 5.20, $^{**}p < 0.01$; CRF versus EtOH, q = 6.21, $p = 0.05$). This
367 suggests that alcohol pretreatment (withdrawal state) attenuates CRF-induced CIN
368 activation and diminishes alcohol's subsequent suppressive effects. Notably, when
369 comparing the change in firing from baseline to CRF application, alcohol pretreatment
370 blunted CRF-induced CIN activation (Fig. 6F; $t_{(18)} = 2.70$, $^{*}p < 0.05$). Together, these
371 findings indicate that both acute alcohol exposure and early withdrawal attenuate CRF-
372 mediated enhancement of CIN firing, supporting the conclusion that alcohol modulates
373 striatal cholinergic signaling.
374

375 **Discussion**

376 This study identifies a circuit in which CRF-positive neurons in the CeA and BNST
377 provide direct input to dorsal striatal CINs that express CRFR1. CRF enhances CIN
378 excitability and ACh release, linking CRF to cholinergic modulation. In addition, alcohol
379 exposure and withdrawal blunt this effect, suggesting that CRF signaling to dorsal striatal
380 CINs may contribute to mechanisms relevant to alcohol use disorder. Using
381 monosynaptic and retrograde circuit tracing, we identified direct projections from CRF-
382 expressing neurons in the CeA and BNST to dorsal striatal CINs. Functional
383 electrophysiology shows that CRF enhances CIN excitability and promotes ACh release
384 via CRFR1 receptors. However, acute alcohol exposure and withdrawal disrupted this

385 excitatory effect, indicating that alcohol interferes with CRF-dependent cholinergic
386 modulation. These findings identify a CRF–CIN circuit that is sensitive to alcohol-induced
387 modulation. Striatal cholinergic signaling is essential for behavioral flexibility [62], and
388 alcohol exposure is known to impair CIN activity and ACh release [49], leading to reduced
389 flexibility. Thus, alcohol-induced alterations in CRF–CIN signaling may disrupt cholinergic
390 control of striatal circuits, providing a potential mechanism by which alcohol promotes
391 cognitive rigidity and compulsive reward-seeking behaviors characteristic of AUD.

392 **Monosynaptic Inputs from the CeA and BNST to CINs**

393 Tracing experiments reported here show that dorsal striatal CINs receive direct
394 synaptic input from CRF-expressing neurons in the CeA and BNST, regions involved in
395 stress and emotion [58, 63]. While previous studies have identified CeA and BNST
396 projections to the striatum, they did not show that they arise from CRF neurons or that
397 they target CINs [52, 64-66]. Our results support the presence of a direct CRF-to-CIN
398 pathway, linking CRF release to cholinergic modulation. Given the role of CINs in striatal
399 output, response flexibility, and reward learning [50, 67-70], this circuit likely contributes
400 to stress-driven behavioral adaptations [58, 71-74]. A limitation of our optogenetic
401 approach is the use of CRF-Cre;Ai32 mice, in which ChR2 is expressed in all CRF+
402 neurons. Thus, although our tracing confirmed CeA and BNST inputs, we cannot exclude
403 contributions from other CRF+ populations. Future work using projection-specific
404 targeting approaches will be required to isolate CeA and BNST contributions.

405 Tracing and receptor expression studies were performed in mice and rats in a
406 largely non-overlapping manner. While mice and rats share many conserved
407 amygdalostriatal components, we did not attempt direct cross-species comparisons, and

408 our findings should therefore be interpreted as species-specific. In rats, CRFR1
409 expression was largely restricted to a subset of CINs, consistent with previous reports. In
410 mice, the histological distribution of CRFR1 remains less well defined; however, our
411 recordings from GFP-labeled CINs in ChAT-GFP mice demonstrated that bath-applied
412 CRF increased CIN firing in a CRFR1-dependent manner. These recordings were
413 conducted in the presence of glutamatergic and GABAergic antagonists, and in some
414 cases TTX, ensuring that CINs were functionally isolated from upstream inputs. Because
415 striatal acetylcholine arises almost exclusively from CINs, with only a minor contribution
416 from brainstem cholinergic afferents, it is most likely that CRF-induced increases in
417 acetylcholine reflect direct CRFR1 signaling in CINs. Nevertheless, the possibility that
418 CRFR1 is expressed in other striatal cell types remains an important open question.
419 Another unresolved question is whether CRFR1+ CINs are equally abundant across
420 striatal subregions. While representative images may appear to suggest higher CRFR1^{+}
421 CIN density in the DLS compared to the DMS, we did not quantify this systematically.
422 Future work will be needed to determine whether such regional differences exist, as they
423 could have important implications for dorsal striatal function.

424 Although CRFR1 expression has been reported in a subset of striatal CINs, we
425 found that the majority of mouse CINs increased firing in response to bath-applied CRF.
426 Using a CRFR1-GFP reporter mouse, only ~10% of CINs showed detectable somatic
427 CRFR1-GFP expression, indicating that widespread CIN responsiveness cannot be
428 explained solely by direct receptor expression at the soma. Reporter lines may
429 underestimate functional CRFR1 expression, particularly if receptors are expressed at
430 low levels or localized to distal neuronal compartments. Consistent with a CRFR1-

431 dependent mechanism, the CRF-induced increase in CIN firing was abolished by a
432 selective CRFR1 antagonist. In addition, CRF may act indirectly by modulating
433 presynaptic inputs to CINs, and electrical coupling among CINs may allow excitation of a
434 subset of neurons to propagate across the network [75]. Together, these mechanisms
435 provide a parsimonious explanation for broad CIN sensitivity to CRF despite limited
436 reporter-detected CRFR1 expression.

437 We found no CRF^+ neurons in the dorsal striatum, indicating that CRF signaling in
438 this region originates from extrinsic inputs, including the CeA and BNST. However, CRF+
439 neurons have been reported in the ventral striatum, where they play a role in learning-
440 related processes [76]. Thus, CRF's contribution to striatal function may differ along the
441 dorsal-ventral axis, with intrinsic ventral striatal CRF^+ neurons complementing extrinsic
442 dorsal striatal CRF inputs. These sources of CRF may modulate striatal circuits involved
443 in selecting behaviors flexibly, a process critical for adaptive responses to stress.
444 Electrophysiological experiments further show that CRF fiber stimulation enhances CIN
445 excitability even in the presence of synaptic blockers, supporting a direct modulatory role
446 for CRF signaling on cholinergic tone in the striatum. Moreover, the transient effects of
447 endogenous CRF release, compared to the prolonged activation from CRF bath
448 application, suggest that CRF signaling may generate temporally dynamic patterns of CIN
449 activity to influence behavioral output.

450 **Alcohol Disrupts CRF-Mediated CIN Excitation**

451 One key observation is that alcohol exposure disrupts CRF-mediated CIN
452 excitation. Both acute alcohol exposure and withdrawal attenuate the CRF-induced
453 increase in CIN activity, indicating that alcohol reduces CIN responsiveness to CRF, a

454 stress-related neuromodulator. Because stress is a well-established trigger for alcohol
455 relapse [77-79], the observed alcohol-induced disruption of CRF signaling may impair the
456 brain's ability to adaptively respond to stress, thereby increasing susceptibility to relapse.
457 Such dysregulation may compromise stress resilience mechanisms normally mediated
458 by CRF–cholinergic interactions within the striatum and related corticostriatal circuits.
459 Under normal stressful conditions, CRF release onto CINs can modulate cholinergic
460 signaling to adjust behavioral strategies and promote flexible adaptation to environmental
461 demands. However, alcohol-induced impairment of CRF–CIN communication and CIN
462 responsiveness may blunt this adaptive flexibility [49, 62]. Consequently, stress may
463 instead bias behavior toward habitual or compulsive alcohol seeking, leading to relapse.
464 These findings highlight a potential pathway through which chronic alcohol exposure
465 erodes adaptive stress coping and promotes relapse vulnerability. While these alcohol
466 effects were modest in magnitude, they were consistent across recordings and
467 statistically reliable. It is important to note, however, that ex vivo slice physiology may
468 underestimate ethanol's impact due to factors such as washout, diffusion barriers, and
469 the absence of an intact network state. Thus, future in vivo studies are needed to evaluate
470 the robustness and behavioral relevance of this modulation. It also remains to be
471 determined whether ethanol pre-exposure alters subsequent CIN responses to ethanol in
472 the absence of CRF, an important question for future studies.
473 One possibility is that alcohol exposure downregulates CRFR1 expression [80, 81] or
474 alters CIN function [49], reducing their responsiveness to stress-related input [82, 83].
475 Another is that alcohol may interfere with intracellular signaling cascades downstream of
476 CRFR1 activation, leading to diminished excitability and ACh release. Another possibility

477 is that alcohol and CRF may converge on CINs through an occlusion mechanism, in which
478 prior activation of CRFR1 reduces the efficacy of subsequent CRF signaling. Although
479 our ex vivo preparation does not readily permit a direct test of this hypothesis, future in
480 vivo approaches with high temporal control will be important to evaluate this possibility.

481 **Implications for Alcohol Use Disorder**

482 By delineating a CRF-to-CIN pathway linking the extended amygdala to the dorsal
483 striatum, our findings provide insight into how stress and alcohol may interact at the circuit
484 level to influence striatal processing relevant to behavior. Given the role of CINs in habit
485 learning and behavioral flexibility [84], disruption of this stress-sensitive cholinergic circuit
486 may underlie the decision-making deficits and compulsive alcohol-seeking behavior
487 observed in AUD [48-50, 85-87].

488 In summary, we identify a direct CRF-positive projection from the CeA and BNST
489 to dorsal striatal CINs, revealing a new mechanism by which stress can modulate
490 cholinergic signaling in the striatum. We show that CRF enhances CIN excitability and
491 ACh release, and that alcohol exposure attenuates this modulation. These findings
492 highlight the CRF-CIN circuit as a potential site of vulnerability in AUD and suggest that
493 restoring CRF signaling may help counteract stress and alcohol-induced striatal
494 dysfunction. Future work should assess whether pharmacological or circuit-based
495 interventions targeting CRFR1 or CINs can mitigate behavioral impairments in individuals
496 with AUD.

497 **Acknowledgements**

498 We thank Yufei Huang for discussions and supplementary data. This research was
499 supported by NIAAA R01AA021505 (JW), R01AA027768 (JW), U01AA025932 (JW),
500 R01MH112768 (NJ), and R21AG086907 (NJ).

501 The authors declare no competing financial interests.

502

503 **References**

504 1. Heilig, M. and G.F. Koob, *A key role for corticotropin-releasing factor in alcohol*
505 *dependence.* Trends in Neurosciences, 2007. 30(8): p. 399–406.
506 2. Becker, H.C., *Effects of Alcohol Dependence and Withdrawal on Stress*
507 *Responsiveness and Alcohol Consumption.* Alcohol Research-Current Reviews,
508 2012. 34(4): p. 448–458.
509 3. Quadros, I.M.H., et al., *An Update on CRF Mechanisms Underlying Alcohol Use*
510 *Disorders and Dependence.* Frontiers in Endocrinology, 2016. 7: p. 134.
511 4. Bruijnzeel, A.W. and M.S. Gold, *The role of corticotropin-releasing factor-like*
512 *peptides in cannabis, nicotine, and alcohol dependence.* Brain Research Reviews,
513 2005. 49(3): p. 505–528.
514 5. Roberto, M., et al., *Corticotropin-Releasing Factor (CRF) and Addictive Behaviors.*
515 International Review of Neurobiology, 2017. 136: p. 5–51.
516 6. Koob, G.F., *Stress, corticotropin-releasing factor, and drug addiction.* Ann N Y
517 Acad Sci, 1999. 897: p. 27–45.
518 7. Haass-Koffler, C.L. and S.E. Bartlett, *Stress and addiction: contribution of the*
519 *corticotropin releasing factor (CRF) system in neuroplasticity.* Front Mol Neurosci,
520 2012. 5: p. 91.
521 8. Koob, G.F., *A role for brain stress systems in addiction.* Neuron, 2008. 59(1): p.
522 11–34.
523 9. Shalev, U., S. Erb, and Y. Shaham, *Role of CRF and other neuropeptides in stress-*
524 *induced reinstatement of drug seeking.* Brain Res, 2010. 1314: p. 15–28.

525 10. Baumgartner, H.M., J. Schulkin, and K.C. Berridge, *Activating Corticotropin-*
526 *Releasing Factor Systems in the Nucleus Accumbens, Amygdala, and Bed*
527 *Nucleus of Stria Terminalis: Incentive Motivation or Aversive Motivation?* Biological
528 Psychiatry, 2021. 89(12): p. 1162–1175.
529 11. Kimchi, E.Y., et al., *Neuronal correlates of instrumental learning in the dorsal*
530 *striatum.* J Neurophysiol, 2009. 102(1): p. 475–89.
531 12. Nonomura, S., et al., *Monitoring and Updating of Action Selection for Goal-*
532 *Directed Behavior through the Striatal Direct and Indirect Pathways.* Neuron, 2018.
533 99(6): p. 1302–1314 e5.
534 13. Redgrave, P., et al., *Goal-directed and habitual control in the basal ganglia:*
535 *implications for Parkinson's disease.* Nat Rev Neurosci, 2010. 11(11): p. 760–72.
536 14. Mantsch, J.R., *Corticotropin releasing factor and drug seeking in substance use*
537 *disorders: Preclinical evidence and translational limitations.* Addict Neurosci, 2022.
538 4.
539 15. Lemos, J.C., J.H. Shin, and V.A. Alvarez, *Striatal cholinergic interneurons are a*
540 *novel target of corticotropin releasing factor.* Journal of Neuroscience, 2019: p.
541 5647–5661.
542 16. Carboni, L., et al., *Increased expression of CRF and CRF-receptors in dorsal*
543 *striatum, hippocampus, and prefrontal cortex after the development of nicotine*
544 *sensitization in rats.* Drug Alcohol Depend, 2018. 189: p. 12–20.
545 17. Abudukeyoumu, N., et al., *Cholinergic modulation of striatal microcircuits.*
546 European Journal of Neuroscience, 2019. 49(5): p. 604–622.

547 18. Tanimura, A., et al., *Striatal cholinergic interneurons and Parkinson's disease.*
548 European Journal of Neuroscience, 2018. 47(10): p. 1148–1158.
549 19. Chantranupong, L., et al., *Dopamine and glutamate regulate striatal acetylcholine*
550 *in decision-making.* Nature, 2023. 621(7979): p. 577.
551 20. Blomeley, C.P., et al., *Ethanol affects striatal interneurons directly and projection*
552 *neurons through a reduction in cholinergic tone.* Neuropsychopharmacology,
553 2011. 36(5): p. 1033–46.
554 21. Lim, S.A., U.J. Kang, and D.S. McGehee, *Striatal cholinergic interneuron*
555 *regulation and circuit effects.* Front Synaptic Neurosci, 2014. 6: p. 22.
556 22. Li, J., et al., *The Orbitofrontal Cortex to Striatal Cholinergic Interneuron Circuit*
557 *Controls Cognitive Flexibility Shaping Alcohol-Seeking Behavior.* Biological
558 Psychiatry, 2025. 97(6): p. 614–626.
559 23. Tallini, Y.N., et al., *BAC transgenic mice express enhanced green fluorescent*
560 *protein in central and peripheral cholinergic neurons.* Physiological Genomics,
561 2006. 27(3): p. 391–7.
562 24. Rossi, J., et al., *Melanocortin-4 receptors expressed by cholinergic neurons*
563 *regulate energy balance and glucose homeostasis.* Cell Metabolism, 2011. 13(2):
564 p. 195–204.
565 25. Ade, K.K., et al., *An Improved BAC Transgenic Fluorescent Reporter Line for*
566 *Sensitive and Specific Identification of Striatonigral Medium Spiny Neurons.*
567 Frontiers in Systems Neuroscience, 2011. 5: p. 32.

568 26. Madisen, L., et al., *A toolbox of Cre-dependent optogenetic transgenic mice for*
569 *light-induced activation and silencing.* Nature Neuroscience, 2012. 15(5): p. 793–
570 802.
571 27. Taniguchi, H., et al., *A resource of Cre driver lines for genetic targeting of*
572 *GABAergic neurons in cerebral cortex.* Neuron, 2011. 71(6): p. 995–1013.
573 28. Weera, M.M., et al., *Generation of a CRF-Cre transgenic rat and the role of central*
574 *amygdala CRF cells in nociception and anxiety-like behavior.* Elife, 2022. 11.
575 29. Pomrenze, M.B., et al., *A Transgenic Rat for Investigating the Anatomy and*
576 *Function of Corticotrophin Releasing Factor Circuits.* Frontiers in Neuroscience,
577 2015. 9: p. 487.
578 30. Lu, J., et al., *Alcohol intake enhances glutamatergic transmission from D2*
579 *receptor-expressing afferents onto D1 receptor-expressing medium spiny neurons*
580 *in the dorsomedial striatum.* Neuropsychopharmacology, 2019. 44(6): p. 1123–
581 1131.
582 31. Wang, J., et al., *Alcohol Elicits Functional and Structural Plasticity Selectively in*
583 *Dopamine D1 Receptor-Expressing Neurons of the Dorsomedial Striatum.* Journal
584 of Neuroscience, 2015. 35(33): p. 11634–43.
585 32. Cheng, Y., et al., *Distinct Synaptic Strengthening of the Striatal Direct and Indirect*
586 *Pathways Drives Alcohol Consumption.* Biological Psychiatry, 2017. 81(11): p.
587 918–929.
588 33. Cheng, Y., et al., *Prenatal Exposure to Alcohol Induces Functional and Structural*
589 *Plasticity in Dopamine D1 Receptor-Expressing Neurons of the Dorsomedial*
590 *Striatum.* Alcoholism: Clinical and Experimental Research, 2018.

591 34. Wei, X., et al., *Dopamine D1 or D2 receptor-expressing neurons in the central*
592 *nervous system.* Addiction Biology, 2018. 23(2): p. 569–584.
593 35. Watabe-Uchida, M., et al., *Whole-brain mapping of direct inputs to midbrain*
594 *dopamine neurons.* Neuron, 2012. 74(5): p. 858–73.
595 36. Klapoetke, N.C., et al., *Independent optical excitation of distinct neural*
596 *populations.* Nat Methods, 2014. 11(3): p. 338–46.
597 37. Oh, S.W., et al., *A mesoscale connectome of the mouse brain.* Nature, 2014.
598 508(7495): p. 207–14.
599 38. Wickersham, I.R., et al., *Monosynaptic restriction of transsynaptic tracing from*
600 *single, genetically targeted neurons.* Neuron, 2007. 53(5): p. 639–47.
601 39. Wang, L., et al., *Characteristics of GABAergic and cholinergic neurons in*
602 *perinuclear zone of mouse supraoptic nucleus.* J Neurophysiol, 2015. 113(3): p.
603 754–67.
604 40. Purvines, W., et al., *Perinatal and prenatal alcohol exposure impairs striatal*
605 *cholinergic function and cognitive flexibility in adult offspring.* Neuropharmacology,
606 2025. 279: p. 110627.
607 41. Huang, Z., et al., *Dynamic responses of striatal cholinergic interneurons control*
608 *behavioral flexibility.* Sci Adv, 2024. 10(51): p. eadn2446.
609 42. Touponse, G.C., et al., *Cholinergic modulation of dopamine release drives effortful*
610 *behavior.* bioRxiv, 2025.
611 43. Potjer, E.V., et al., *Parkinsonian striatal acetylcholine dynamics are refractory to L-*
612 *DOPA treatment.* bioRxiv, 2025.

613 44. Gangal, H., et al., *Traumatic brain injury exacerbates alcohol consumption and*
614 *neuroinflammation with decline in cognition and cholinergic activity.* Transl
615 Psychiatry, 2025. 15(1): p. 403.
616 45. Jing, M., et al., *An optimized acetylcholine sensor for monitoring in vivo cholinergic*
617 *activity.* Nat Methods, 2020. 17(11): p. 1139–1146.
618 46. Ma, T., et al., *Bidirectional and long-lasting control of alcohol-seeking behavior by*
619 *corticostriatal LTP and LTD.* Nature Neuroscience, 2018. 21(3): p. 373–383.
620 47. Hellard, E.R., et al., *Optogenetic control of alcohol-seeking behavior via the*
621 *dorsomedial striatal circuit.* Neuropharmacology, 2019. 155: p. 89–97.
622 48. Gangal, H., et al., *Drug reinforcement impairs cognitive flexibility by inhibiting*
623 *striatal cholinergic neurons.* Nature Communications, 2023. 14(1): p. 3886.
624 49. Ma, T., et al., *Chronic alcohol drinking persistently suppresses thalamostriatal*
625 *excitation of cholinergic neurons to impair cognitive flexibility.* Journal of Clinical
626 Investigation, 2022. 132(4): p. e154969.
627 50. Huang, Z., et al., *Dynamic responses of striatal cholinergic interneurons control*
628 *behavioral flexibility.* Science Advances, 2024. 10(51): p. eadn2446.
629 51. de Guglielmo, G., et al., *Inactivation of a CRF-dependent amygdalofugal pathway*
630 *reverses addiction-like behaviors in alcohol-dependent rats.* Nature
631 Communications, 2019. 10(1): p. 1238.
632 52. Lu, J.Y., et al., *Whole-Brain Mapping of Direct Inputs to Dopamine D1 and D2*
633 *Receptor-Expressing Medium Spiny Neurons in the Posterior Dorsomedial*
634 *Striatum.* Eneuro, 2021. 8(1).

635 53. Paxinos, G., C.R. Watson, and P.C. Emson, *AChE-stained horizontal sections of*
636 *the rat brain in stereotaxic coordinates.* Journal of Neuroscience Methods, 1980.
637 3(2): p. 129–49.
638 54. Franklin, K.B.J. and G. Paxinos, *The mouse brain in stereotaxic coordinates*. 3 ed.
639 2007, San Diego: Academic Press.
640 55. Ma, T., et al., *Alcohol induces input-specific aberrant synaptic plasticity in the rat*
641 *dorsomedial striatum.* Neuropharmacology, 2017. 123: p. 46–54.
642 56. Davis, M., *Neural systems involved in fear and anxiety measured with fear-*
643 *potentiated startle.* American Psychologist, 2006. 61(8): p. 741–756.
644 57. Funk, C.K., et al., *Corticotropin-releasing factor within the central nucleus of the*
645 *amygdala mediates enhanced ethanol self-administration in withdrawn, ethanol-*
646 *dependent rats.* Journal of Neuroscience, 2006. 26(44): p. 11324–11332.
647 58. Partridge, J.G., et al., *Stress increases GABAergic neurotransmission in CRF*
648 *neurons of the central amygdala and bed nucleus stria terminalis.*
649 Neuropharmacology, 2016. 107: p. 239–250.
650 59. Sanford, C.A., et al., *A Central Amygdala CRF Circuit Facilitates Learning about*
651 *Weak Threats.* Neuron, 2017. 93(1): p. 164–178.
652 60. Chen, A., *Genetic Dissection of the Neuroendocrine and Behavioral Responses to*
653 *Stressful Challenges*, in *Stem Cells in Neuroendocrinology*, D. Pfaff and Y.
654 Christen, Editors. 2016: Cham (CH). p. 69–79.
655 61. Olson, K.L., et al., *Cholinergic interneurons in the nucleus accumbens are a site*
656 *of cellular convergence for corticotropin-releasing factor and estrogen regulation*

657 *in male and female mice.* European Journal of Neuroscience, 2024. 60(5): p.
658 4937–4953.
659 62. Matamales, M., et al., *Aging-Related Dysfunction of Striatal Cholinergic*
660 *Interneurons Produces Conflict in Action Selection.* Neuron, 2016. 90(2): p. 362–
661 73.
662 63. Kim, S.Y., et al., *Diverging neural pathways assemble a behavioural state from*
663 *separable features in anxiety.* Nature, 2013. 496(7444): p. 219–23.
664 64. Giovanniello, J.R., et al., *A dual-pathway architecture for stress to disrupt agency*
665 *and promote habit.* Nature, 2025.
666 65. Smith, J.B., et al., *Genetic-Based Dissection Unveils the Inputs and Outputs of*
667 *Striatal Patch and Matrix Compartments.* Neuron, 2016. 91(5): p. 1069–1084.
668 66. Heaton, E.C., et al., *Control of goal-directed and inflexible actions by dorsal striatal*
669 *melanocortin systems, in coordination with the central nucleus of the amygdala.*
670 Progress in Neurobiology, 2024. 238: p. 102629.
671 67. Duhne, M., et al., *A mismatch between striatal cholinergic pauses and*
672 *dopaminergic reward prediction errors.* Proceedings of the National Academy of
673 Sciences of the United States of America, 2024. 121(41): p. e2410828121.
674 68. Ostlund, S.B., et al., *Modulation of cue-triggered reward seeking by cholinergic*
675 *signaling in the dorsomedial striatum.* European Journal of Neuroscience, 2017.
676 45(3): p. 358–364.
677 69. Dautan, D., et al., *Cholinergic midbrain afferents modulate striatal circuits and*
678 *shape encoding of action strategies.* Nature Communications, 2020. 11(1): p.
679 1739.

680 70. Aoki, S., et al., *Cholinergic interneurons in the rat striatum modulate substitution*
681 *of habits.* European Journal of Neuroscience, 2018. 47(10): p. 1194–1205.
682 71. Rieger, N.S., et al., *Insular cortex corticotropin-releasing factor integrates stress*
683 *signaling with social affective behavior.* Neuropsychopharmacology, 2022. 47(6):
684 p. 1156–1168.
685 72. Alizamini, M.M., et al., *Corticotropin-releasing factor receptor 1 in infralimbic cortex*
686 *modulates social stress-altered decision-making.* Progress in Neuro-
687 Psychopharmacology & Biological Psychiatry, 2022. 116: p. 110523.
688 73. Bryce, C.A. and S.B. Floresco, *Perturbations in Effort-Related Decision-Making*
689 *Driven by Acute Stress and Corticotropin-Releasing Factor.*
690 Neuropsychopharmacology, 2016. 41(8): p. 2147–59.
691 74. Pomrenze, M.B., et al., *A Corticotropin Releasing Factor Network in the Extended*
692 *Amygdala for Anxiety.* Journal of Neuroscience, 2019. 39(6): p. 1030–1043.
693 75. Ren, Y., Y. Liu, and M. Luo, *Gap Junctions Between Striatal D1 Neurons and*
694 *Cholinergic Interneurons.* Front Cell Neurosci, 2021. 15: p. 674399.
695 76. Eckenwiler, E.A., et al., *Corticotropin-Releasing Factor Release From a Unique*
696 *Subpopulation of Accumbal Neurons Constrains Action-Outcome Acquisition in*
697 *Reward Learning.* Biol Psychiatry, 2025. 97(6): p. 637–650.
698 77. Bertotto, M.E., et al., *Increased voluntary ethanol consumption and c-Fos*
699 *expression in selected brain areas induced by fear memory retrieval in ethanol*
700 *withdrawn rats.* European Neuropsychopharmacology, 2010. 20(8): p. 568–81.

701 78. Becker, H.C., et al., *Oxytocin Reduces Sensitized Stress-Induced Alcohol Relapse*
702 *in a Model of Posttraumatic Stress Disorder and Alcohol Use Disorder*
703 *Comorbidity.* Biological Psychiatry, 2023. 94(3): p. 215–225.
704 79. Walker, L.C., H.E. Kastman, and A.J. Lawrence, *Pattern of neural activation*
705 *following yohimbine-induced reinstatement of alcohol seeking in rats.* European
706 Journal of Neuroscience, 2020. 51(3): p. 706–720.
707 80. Hansson, A.C., et al., *Region-specific down-regulation of gene expression in*
708 *alcohol-preferring msP rats following access to alcohol.* Addiction Biology, 2007.
709 12(1): p. 30–34.
710 81. Zhou, Y., et al., *Reduced hypothalamic POMC and anterior pituitary CRF1 receptor*
711 *mRNA levels after acute, but not chronic, daily "binge" intragastric alcohol*
712 *administration.* Alcoholism: Clinical and Experimental Research, 2000. 24(10): p.
713 1575–82.
714 82. Besheer, J., et al., *Stress hormone exposure reduces mGluR5 expression in the*
715 *nucleus accumbens: functional implications for interoceptive sensitivity to alcohol.*
716 Neuropsychopharmacology, 2014. 39(10): p. 2376–86.
717 83. Sayette, M.A., et al., *A test of the appraisal-disruption model of alcohol and stress.*
718 Journal of Studies on Alcohol, 2001. 62(2): p. 247–256.
719 84. Bradfield, L.A., et al., *The thalamostriatal pathway and cholinergic control of goal-*
720 *directed action: interlacing new with existing learning in the striatum.* Neuron, 2013.
721 79(1): p. 153–66.

722 85. Zorrilla, E.P., M.L. Logrip, and G.F. Koob, *Corticotropin releasing factor: a key role*
723 *in the neurobiology of addiction.* Frontiers in Neuroendocrinology, 2014. 35(2): p.
724 234–44.
725 86. Moberg, C.A., et al., *Increased startle potentiation to unpredictable stressors in*
726 *alcohol dependence: Possible stress neuroadaptation in humans.* Journal of
727 Abnormal Psychology, 2017. 126(4): p. 441–453.
728 87. Koob, G.F. and L. Vendruscolo, *Theoretical Frameworks and Mechanistic Aspects*
729 *of Alcohol Addiction: Alcohol Addiction as a Reward Deficit/Stress Surfeit Disorder.*
730 Current Topics in Behavioral Neurosciences, 2023.

731

732 **Figure Legends**

733 **Figure 1. Dorsal Striatal CINs Receive Monosynaptic Inputs From the CeA and**

734 **BNST**

735 **A,** Schematic illustrating the infusion of helper viruses (AAV-DIO-TVA-mCherry and AAV-

736 DIO-RG) and rabies-GFP (RV-GFP) into the dorsal striatum of ChAT-Cre;D1-tdTomato

737 mice. The rabies-GFP was infused 3 weeks after the helper virus infusion, and animals

738 were euthanized one week after the rabies infusion. **B,** Model for the retrograde

739 transsynaptic labeling of CeA and BNST neurons projecting to dorsal striatal CINs. TVA

740 permits selective infection by the rabies-GFP virus, while RG mediates the retrograde

741 transsynaptic jump from postsynaptic CINs to presynaptic terminals of CeA or BNST

742 neurons. **C,** Sample image showing CeA neurons projecting to dorsal striatal CINs, as

743 indicated by rabies-GFP expression. AP: -1.50 mm from Bregma. TS, tail of the striatum.

744 Scale bar: 0.5 mm, 50 μm for insert. **D,** Sample image demonstrating that BNST neurons

745 project to dorsal striatal CINs, as indicated by rabies-GFP expression. Note that the

746 injection site (inj. site) is also displayed in the posterior dorsal striatum. AP: -0.26 mm

747 from Bregma. DS, dorsal striatum; ac, anterior commissure. Scale bar: 0.5 mm, 50 μm

748 for insert. **E,** The CeA and BNST both send projections to the dorsal striatum, with the

749 BNST providing more inputs. ***$p < 0.001$ by Mann-Whitney test. n = 13 sections from 4

750 mice (13/4) for the CeA and 15/4 for the BNST.

751

752

753 **Figure 2. CRF-Positive Neurons Are Abundant in the CeA and BNST but Absent in**
754 **the Dorsal Striatum**

755 **A**, **B,** Confocal images showing dense populations of tdTomato-labeled CRF^+ neurons in
756 the CeA (A) and BNST (B) of CRF-Cre;tdTomato rats. AP: -1.5 mm from Bregma (A) and
757 -0.26 mm (B). Scale bars: 1 mm (left) and 50 μm (right). DS, dorsal striatum. **C**,
758 Representative image of the posterior dorsal striatum showing the presence of CRF^+
759 axonal fibers but the absence of CRF^+ cell bodies. AP: -0.26 mm from Bregma. Scale bar:
760 100 μm. **D**, The CeA and BNST contain more CRF^+ neurons than the dorsal striatum. *p
761 < 0.05 by Kruskal-Wallis with Dunn's Method. n = 20 slices from 7 rats (20/7) for the CeA,
762 29/7 for the striatum, and 15/7 for the BNST.

763

764

765 **Figure 3. CINs Receive Monosynaptic Input From CeA and BNST CRF^+ Neurons**

766 **A,** Schematic showing virus injection (AAVretro-DIO-GFP) into the dorsal striatum of
767 CRF-Cre;tdTomato rats. **B,** Representative image showing the injection site of AAVretro-
768 DIO-GFP in the posterior dorsal striatum of CRF-Cre;tdTomato rats. Overlapping
769 $tdTomato^+$ (CRF^+) and dorsal striatum-derived Cre-driven GFP^+ expression in the BNST
770 (depicted in yellow) indicates that these CRF^+ neurons project to the dorsal striatum. ac**,**
771 anterior commissure; LV**,** left ventricle; tdT**,** tdTomato; DS-proj, dorsal-striatum-projecting.
772 Scale bar: 0.5 mm (left), 10 μm (right). The AP coordinates for the injection site from each
773 of the 5 rats are as follows: AP: 0.00 mm, 0.10 mm, 0.12 mm, 0.00 mm, 0.11 mm. **C,**
774 Images showing the overlap (in yellow) of $tdTomato^+$ (CRF^+) and dorsal striatum-derived
775 Cre-driven GFP^+ expression in the CeA, confirming that these CRF^+ neurons also project
776 to the dorsal striatum. TS**,** the tail of the striatum. Scale bar: 1 mm (left), 10 μm (right). **D,**

777 The CeA and BNST contain a similar CRF$^+$ neuron density. n.s., not significant, $p > 0.05$
778 by unpaired t test, n = 9 sections from 5 rats (9/5) for the CeA and 8/5 for the BNST. **E,**
779 The proportion of CRF$^+$ neurons projecting to the dorsal striatum is higher in the BNST
780 compared to the CeA. ***$p < 0.001$ by unpaired t test, n = 9/5 (CeA) and 8/5 (BNST). **F,**
781 The density of dorsal striatum-projecting CRF$^+$ neurons is greater in the BNST than the
782 CeA. **$p < 0.01$. n = 9/5 (CeA) and 8/5 (BNST). **G,** Schematic showing the injection of
783 AAV-FLEX-Chrimson-tdTomato into the CeA and BNST of CRF-Cre;ChAT-eGFP mice
784 and the subsequent recording of green striatal CINs during blue light stimulation of
785 surrounding Chrimson-containing fibers from CRF$^+$ neurons. Fibers were stimulated at a
786 wavelength of 590 nm for 2 ms. **H,** Sample traces showing CIN responses to blue light
787 stimulation of CRF fibers, which were abolished by TTX, recovered with TTX+4-AP and
788 further eliminated by bicuculline (Bic). **I,** Summary of oIPSC data showing the
789 disappearance of oIPSCs with TTX and reappearance with TTX and 4-AP. *$p < 0.05$ by
790 one-way ANOVA. n = 4 slices. **J,** The average latency between the start of optogenetic
791 stimulation and postsynaptic response was ~6.5 ms. n = 8 cells.
792
793
794 **Figure 4. CRFR1 is Expressed in Striatal CINs**
795 **A**, Representative image of a coronal striatal section from a CRFR1-Cre-tdTomato rat
796 showing CRFR1 expression overlapping with anti-ChAT immunoreactivity. The section
797 was stained using an anti-ChAT antibody and imaged using a far-red (647 nm)
798 wavelength (white). Scale bars: 1 mm (left), 100 µm (middle), and 20 µm (right). **B,** There
799 are significantly fewer CRFR1$^+$ CINs than the total number of CINs in the dorsal striatum.
800 ***$p < 0.001$ by Mann-Whitney test. n = 8 sections from 2 rats. **C,** Around 30% of CINs

801 express CRFR1 in CRFR1-Cre;tdT rat. n = 8 sections from 2 rats. **D**, Representative
802 image of a coronal striatal section from a CRFR1-GFP mouse showing CRFR1
803 expression overlapping with anti-ChAT immunoreactivity. **E**, Around 9% of CINs express
804 CRFR1 in CRFR1-GFP mouse. n = 35 sections from 4 mice.
805
806
807 **Figure 5. CRF Enhances CIN Activity and ACh Release in the Dorsal Striatum**
808 **A**, Sample images of GFP-labeled CINs in the striatum of a ChAT-eGFP mouse. Scale
809 bar: 0.5 mm, 50 μm (inset). **B**, Bath application of CRF (100 nM) increased the
810 spontaneous firing of dorsal striatal CINs in cell-attached electrophysiological recordings.
811 This effect was prevented by pretreatment with the CRFR1 antagonist NBI 35695 (5 μM).
812 n = 7 cells from 3 mice (7/3) for CRF and 6/3 for CRF plus antagonist recordings. **C,** Data
813 showing that CRF significantly increases the firing from baseline and the firing frequency
814 in the presence of CRF following pretreatment with CRFR1 antagonist is significantly
815 lower. ***$p < 0.001$ by paired t-test, ***$p < 0.001$ by Mann Whitney test. n = 7 cells from 3
816 mice. **D,** Sample images of ACh sensor fluorescence in dorsal striatal slices before and
817 during bath application of CRF (100 nM). AAV-hSyn-GRAB$_{ACh4m}$ (BrainVTA) was infused
818 into the dorsal striatum of wildtype mice, and live-tissue confocal imaging was conducted
819 two weeks post-infusion. Scale bar: 10 μm for left and right. **E,** Sample trace of
820 spontaneous ACh release events (indicated by red arrows, top). Bath application of CRF
821 increased ACh sensor fluorescence (bottom). **F,** Summary data showing a significant
822 increase in ACh sensor fluorescence following CRF application. *$p < 0.05$ by Mann-
823 Whitney test. n = 7 slices from 7 mice. **G,** Schematic of cell-attached electrophysiological

824 recordings from dorsal striatal CINs in CRF-Cre;Ai32;ChAT-eGFP mice, with
825 simultaneous optogenetic stimulation of CRF^+ fibers using blue light (470-nm, 2 ms, 50
826 Hz, 60 sec). **H,** Sample trace showing the increase in CIN firing frequency during blue
827 light stimulation of CRF^+ fibers. **I,** Data demonstrating a significant and reversible increase
828 in CIN firing frequency during optogenetic stimulation, $*p < 0.05$, $***p < 0.001$ by one-way
829 RM ANOVA. n = 13 neurons from 8 animals. **J**, Sample trace showing no change in CIN
830 firing frequency during blue light stimulation of CRF^+ fibers when CRFR1 antagonist
831 (antalarmin hydrochloride, 2 μM) was bath applied. **I**, Data demonstrating no significant
832 change in Cin firing frequency during optogenetic stimulation. n = 9 neurons from 3 mice.
833

834 **Figure 6. Acute Alcohol Exposure Attenuates CRF-Induced Enhancement of CIN**
835 **Activity**

836 **A,** Time course of spontaneous firing in CINs from dorsal striatal slices of ChAT-eGFP
837 mice, before, during, and after bath application of alcohol (EtOH; 50 mM). **B,** Summary
838 data demonstrates a significant reduction in CIN firing frequency following alcohol
839 application. $**p < 0.01$ by Mann-Whitney test. n = 6 cells from 4 mice. **C,** Schematic of the
840 experimental design in which striatal slices were pretreated with alcohol (50 mM) for 1 h
841 in an incubation chamber and then washed for 15 min in the recording chamber. CINs
842 were selected for cell-attached electrophysiological recordings, measuring firing
843 frequency for 10 min (baseline), followed by CRF (40 nM) and alcohol (50 mM) bath
844 applications for 10 min each. **D, E,** Data showing spontaneous firing of CINs during
845 baseline (BL), CRF, and alcohol bath application for the control (D) and alcohol pretreated
846 (E) groups. $*p < 0.05$, $**p < 0.01$, $***p < 0.001$ by one-way RM ANOVA. n = 10 cells from
847 8 mice (10/8) for the control group and 10/7 for the alcohol pretreated group. **F,** Data

848 showing that alcohol pretreatment attenuated CRF-induced enhancement of CIN firing
849 frequency. *$p < 0.05$ by unpaired t-test. n = 10 cells from 8 mice (10/8) for the control
850 group and 10/7 for the pretreated group.

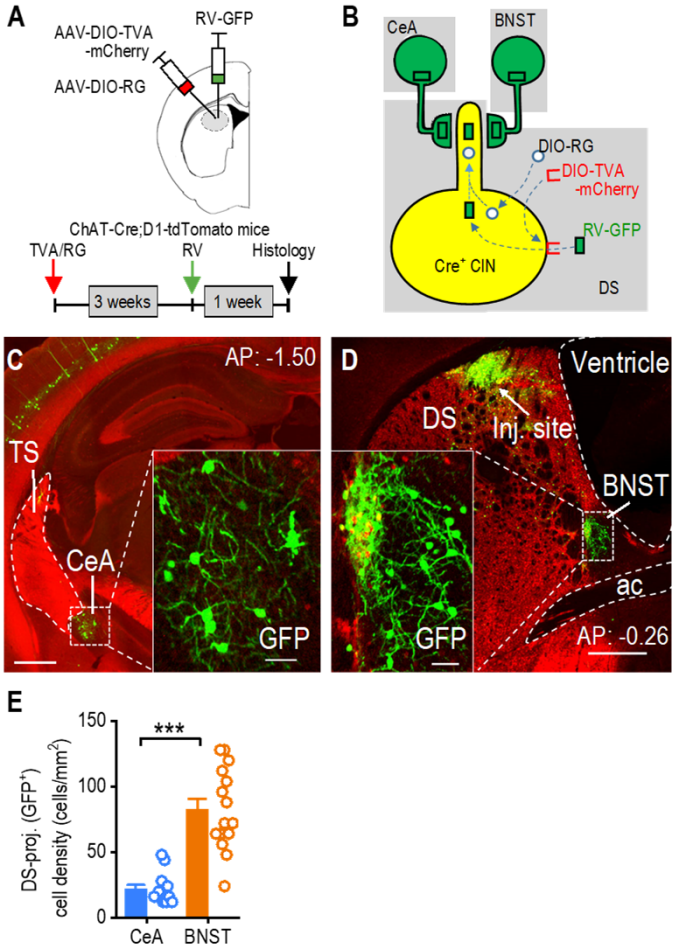
A
AAV-DIO-TVA
-mCherry
RV-GFP
AAV-DIO-RG
ChAT-Cre;D1-tdTomato mice
TVA/RG
RV
Histology
3 weeks
1 week
B
CeA
BNST
DIO-RG
DIO-TVA
-mCherry
RV-GFP
Cre+ CIN
DS
C
AP: -1.50
TS
CeA
GFP
D
Ventricle
DS
Inj. site
BNST
ac
GFP
AP: -0.26
E
DS-proj. (GFP+)
cell density (cells/mm2)
150
100
50
0
***
CeA
BNST

Figure 1

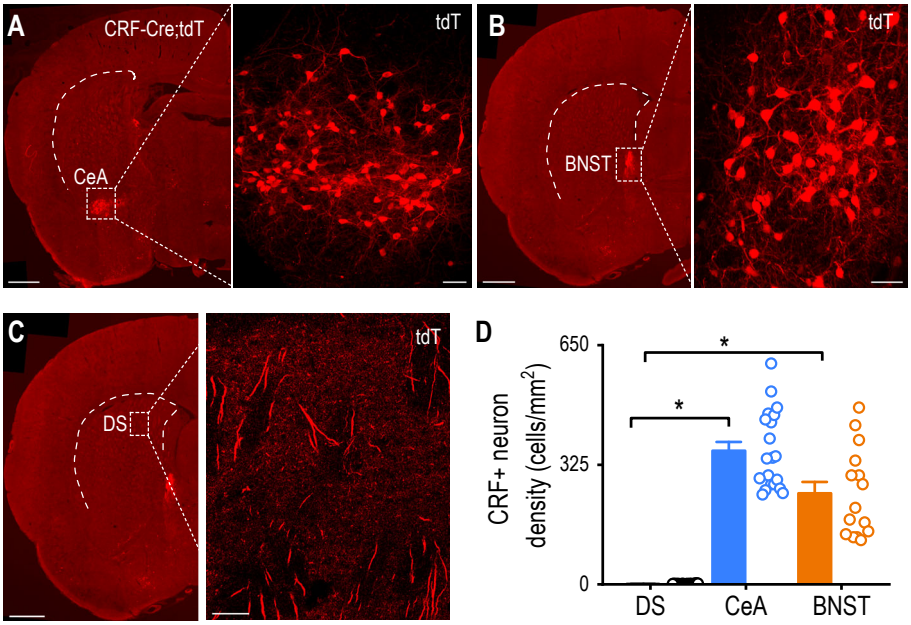
A
CRF-Cre;tdT
CeA
tdT
B
BNST
tdT
C
DS
tdT
D
CRF+ neuron density (cells/mm2)
650
325
0
*
*
DS
CeA
BNST

Figure 2

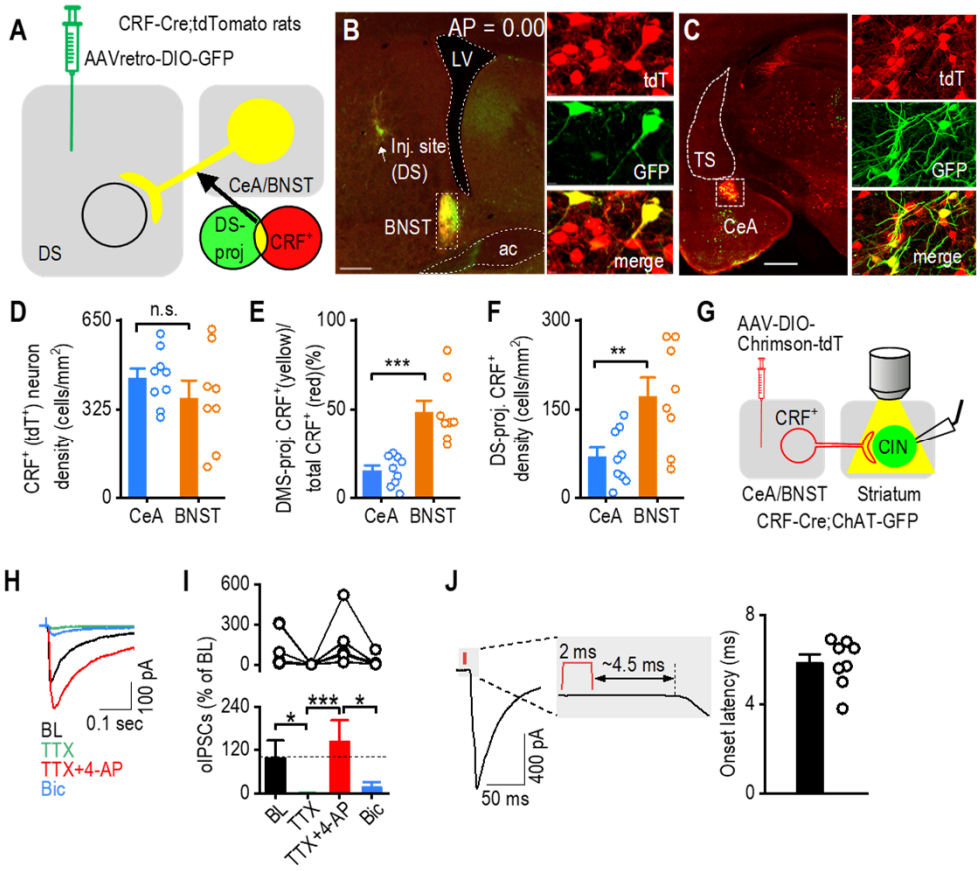
A
CRF-Cre;tdTomato rats
AAVretro-DIO-GFP
CeA/BNST
DS
DS-proj
CRF+
B
AP = 0.00
LV
Inj. site (DS)
BNST
ac
tdT
GFP
merge
C
TS
CeA
tdT
GFP
merge
D
n.s.
CRF+ (tdT+) neuron density (cells/mm2)
650
325
0
CeA
BNST
E
***
DMS-proj. CRF+(yellow)/ total CRF+ (red)(%)
100
50
0
CeA
BNST
F
**
DS-proj. CRF+ density (cells/mm2)
300
150
0
CeA
BNST
G
AAV-DIO-Chrimson-tdT
CRF+
CIN
CeA/BNST
Striatum
CRF-Cre;ChAT-GFP
H
100 pA
0.1 sec
BL
TTX
TTX+4-AP
Bic
I
600
300
0
oIPSCs (% of BL)
240
120
0
*
***
*
BL
TTX
TTX+4-AP
Bic
J
2 ms
~4.5 ms
400 pA
50 ms
Onset latency (ms)
8
4
0

Figure 3

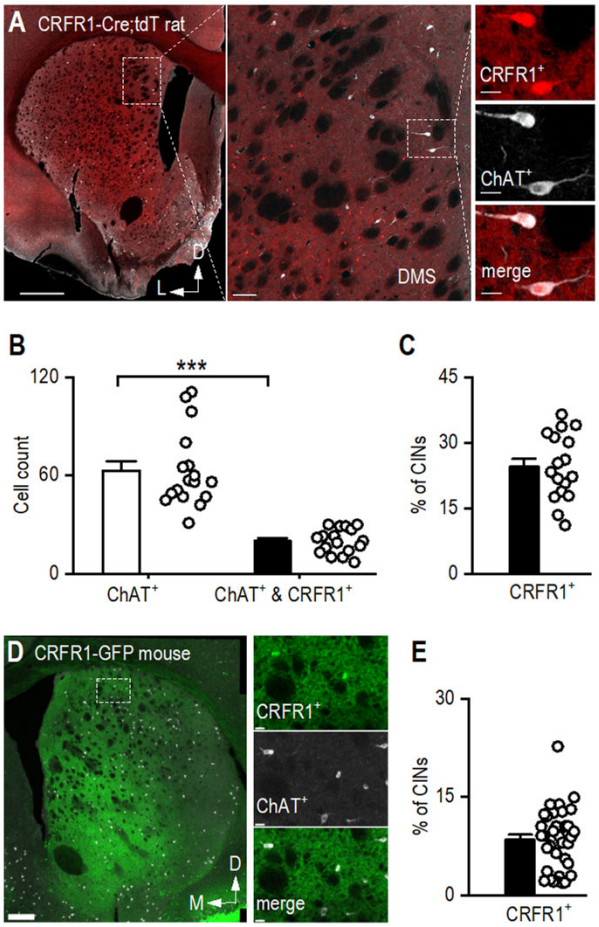
A
CRFR1-Cre;tdT rat
D
L
DMS
CRFR1+
ChAT+
merge
B
***
120
60
0
Cell count
ChAT+
ChAT+ & CRFR1+
C
45
30
15
0
% of CINs
CRFR1+
D
CRFR1-GFP mouse
D
M
CRFR1+
ChAT+
merge
E
30
15
0
% of CINs
CRFR1+

Figure 4

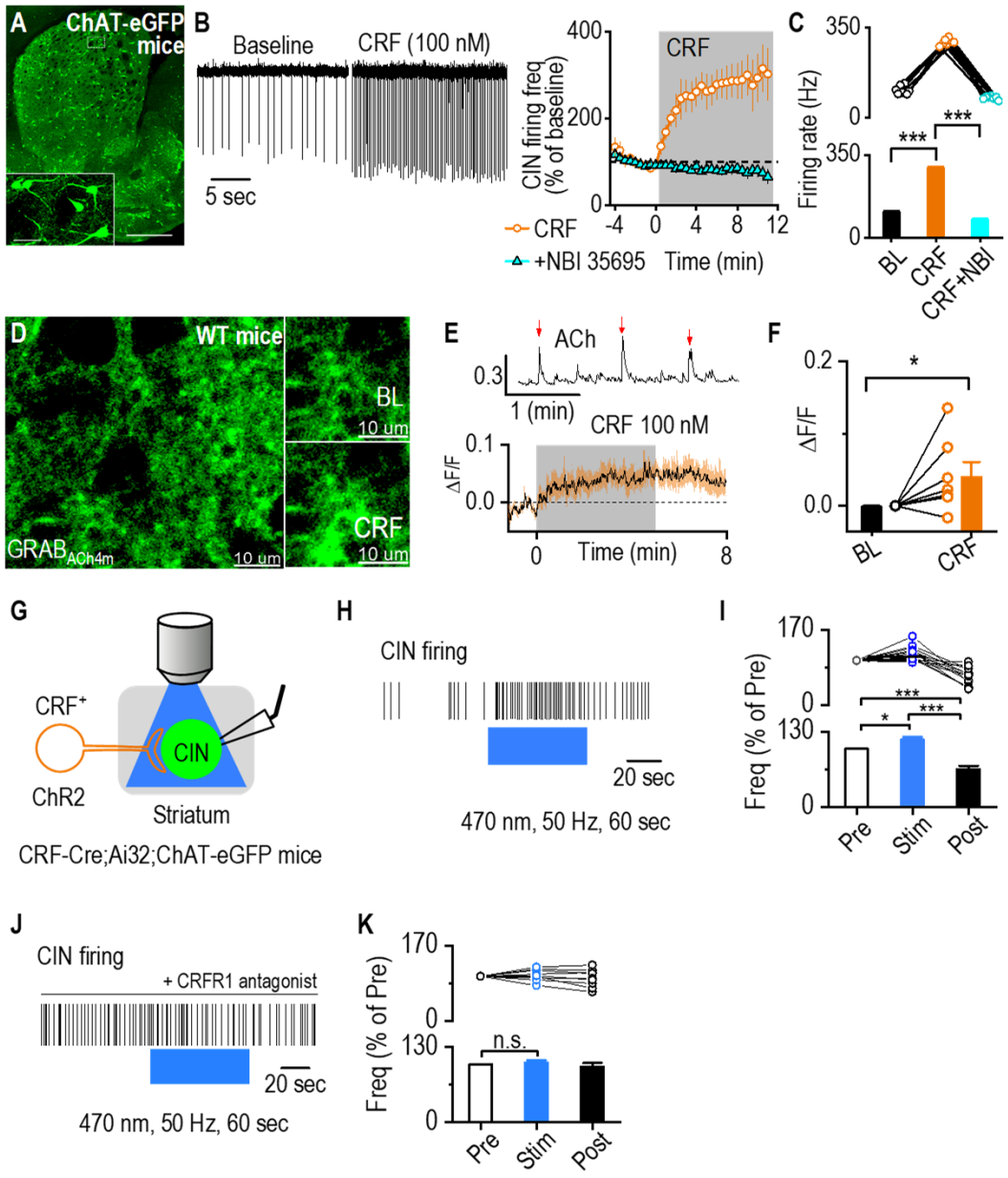
A
ChAT-eGFP mice
B
Baseline
CRF (100 nM)
5 sec
CIN firing freq (% of baseline)
400
200
0
CRF
-4
0
4
8
12
CRF
+NBI 35695
Time (min)
C
350
0
Firing rate (Hz)
***
***
BL
CRF
CRF+NBI
D
WT mice
BL
10 um
CRF
10 um
GRAB ACh4m
10 um
E
ACh
0.3
1 (min)
CRF 100 nM
0.1
0.0
ΔF/F
0
Time (min)
8
F
0.2
0.0
ΔF/F
*
BL
CRF
G
CRF+
CIN
ChR2
Striatum
CRF-Cre;Ai32;ChAT-eGFP mice
H
CIN firing
20 sec
470 nm, 50 Hz, 60 sec
I
170
0
130
0
Freq (% of Pre)
***
*
***
Pre
Stim
Post
J
CIN firing
+ CRFR1 antagonist
20 sec
470 nm, 50 Hz, 60 sec
K
170
0
130
0
Freq (% of Pre)
n.s.
Pre
Stim
Post

Figure 5

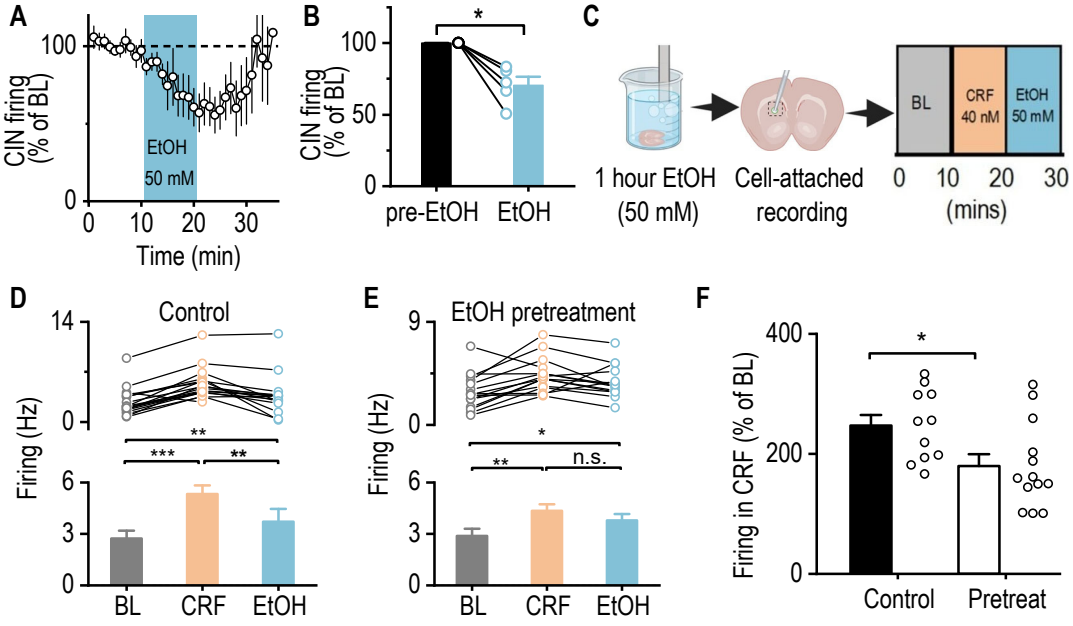
A
100
0
CIN firing (% of BL)
EtOH
50 mM
0
10
20
30
Time (min)
B
*
100
50
0
CIN firing (% of BL)
pre-EtOH
EtOH
C
1 hour EtOH (50 mM)
Cell-attached recording
BL
CRF 40 nM
EtOH 50 mM
0
10
20
30
(mins)
D
Control
14
0
Firing (Hz)
**
***
**
6
3
0
BL
CRF
EtOH
E
EtOH pretreatment
9
0
Firing (Hz)
*
**
n.s.
6
3
0
BL
CRF
EtOH
F
400
200
0
Firing in CRF (% of BL)
*
Control
Pretreat

Figure 6